Hindawi
Journal of Nanomaterials
Volume 2022, Article ID 5735757, 13 pages
https://doi.org/10.1155/2022/5735757

Research Article

Application of Nanoscale Microparticle Technology in Medical Imaging Diagnosis and Treatment

Jingzhe Li

College of Nursing, Hebi Polytechnic, Hebi, Henan, China 458030

Correspondence should be addressed to Jingzhe Li; 2111820011@e.gzhu.edu.cn

Received 24 March 2022; Revised 22 June 2022; Accepted 4 July 2022; Published 30 July 2022

Academic Editor: Awais Ahmed

Nanotechnology is an alternative material manufacturing technology, and the research field involves a broad field of modern technology, especially in the field of high-end manufacturing. Nanotechnology is a technique for studying the properties and applications of materials with structural dimensions in the range of 1 nanometer to 100 nanometers. Medical imaging refers to the technology and processing process of obtaining internal tissue images of the human body or a certain part of the human body in a noninvasive way for medical treatment or medical research; the acquired image can be further processed to restore the original image that was not clear enough to highlight some characteristic information in the image. The appearance of medical imaging has promoted the development of the medical field. The purpose of this paper is to study the application of nanoscale microparticle technology in medical imaging diagnosis and treatment. It is expected that the combination of nanotechnology and medical imaging will improve the accuracy of medical imaging diagnosis. This paper mainly introduces the general methods and technologies of technical development of medical imaging instruments and briefly shows the process of data and image analysis. The experimental results in this paper show that when other conditions remain unchanged, the image quality will change when the quality factor of the image changes. When the image quality is 60%, the image transmission rate is about 5.5FPS, which is relatively stable and can be used in the medical field.

1. Introduction

With the continuous rise of science, all fields of society have developed rapidly, and scientific research has reached the level of microscopic molecules, providing new possibilities for scientific research. The development and popularization of medical imaging technology and the substantial improvement of computer computing power have greatly promoted the development of medical image processing technology. With the continuous development of nanotechnology, a large number of nanomaterials appear in the field of social production and are widely used in the biological field. When nanobiology develops to a certain technology, nanomaterials can be used to make nanobiological cells with recognition ability, and the biomedicine of cancer cells can be absorbed and injected into the human body, which can be used for targeted killing of cancer cells. With the improvement of living standards, people pay more and more attention to their own health. How to combine nanotechnology and medical imaging technology to improve the level of medical diagnosis is a problem that should be considered at present. Since the development of medical imaging, in addition to X-ray, there are other imaging technologies. In terms of information application, image files and image digitized files can be exchanged and viewed, and the medical digital image transmission protocol technology has been developed.

The combination of medical imaging and nanotechnology can accurately extract images of lesions, reduce manual workload, improve image extraction speed, and make diagnosis results more accurate. Combining multiple imaging modes to achieve complementary advantages of each imaging mode is of great significance in biomedical imaging.

The combination of the two further enhances the digitization of hospitals and drives the development of the biomedical industry.

In this paper, an evaluation version of the X-ray medical imaging diagnostic instrument is designed, which provides the conditions for the secondary development to realize the digital acquisition and diagnosis of medical imaging data. In this paper, an image compression algorithm based on adaptive truncation coding is proposed, which solves the problem that excessive coding of unimportant coefficients brings workload to image compression.

2. Related Work

The broad application of nanotechnology in the biological field provides the possibility for the development of the medical field. Image-guided core needle biopsy is an important tool in the treatment of musculoskeletal tumors. Although the diagnostic yield and accuracy of this procedure are high, nondiagnostic results may occur. Nondiagnostic CNB results can cause unnecessary anxiety and can lead to repeat biopsies and delays in treatment. The Chinese name of CNB is fine needle biopsy, which refers to taking biopsies from the body for pathological examination, that is, observing cell morphology and the relationship between cells under a microscope. Lin et al. believe that understanding the radiological and histological factors that affect the diagnostic rate of CNB in musculoskeletal lesions can help radiologists select lesion sites for biopsy and help manage physician and patient expectations for biopsy results. Informing radiologists about the factors associated with low diagnostic rates during CNB of musculoskeletal lesions can improve diagnostic rates, demonstrating that this technique can be used in diagnosis [1]. Medical imaging is the foundation of child care, and much of the field of medical imaging relies on ionizing radiation: radiography, fluoroscopy, CT, and nuclear imaging. Frush and Sorantin believe that many considerations for this imaging of children differ in terms of appropriate radiation use, other factors that determine examination quality, opportunities for participation and education through the Internet, and translation of research work. Given these needs, it is imperative to explore the contribution of the pediatric radiology community and its impact, especially in improving the value of children's care [2]. Exposure to low-dose radiation has increased exponentially due to the influx of diagnostic imaging and medical procedures that use radiation, and this set dose limit essentially limits the use of medical radiation for diagnosis due to public health concerns. Low-dose radiation refers to ionizing radiation with a low energy transfer linear density at a dose of 100 mSv and below, and its main health risk is random effects. Rpsgt investigated radiation exposure concerns in the form of a retrospective review of previous experimental studies and an observational evaluation of the health effects of low-dose radiation. These studies show that high doses of ionizing radiation have toxic effects and increase cancer risk. Furthermore, the limitations of radiation in medical imaging are based on the assumption that the health risk of low-dose radiation is a linear extrapolation of high-dose radiation [3]. Mobile devices and software now have sufficient computing power, speed, and complexity to interpret radiology examinations in real time. Venson et al. conducted a multivariate user study exploring image-based diagnostic capabilities using mobile devices and traditional workstations. Using CT, MRI, and radiographic datasets, they performed a task analysis between subjects, showing that for images from emergency mode, a mobile interface can provide accurate interpretation and rapid response, which may benefit patient healthcare [4]. As technology nodes shrink below 45 nm, high power issues have become a major disadvantage of CMOS logic circuits. Emerging spintronic nanodevice-based hybrid memory logic architectures have recently been investigated to overcome these issues. Deng et al. conducted a research on the architecture design of multicontext hybrid STT-MTJ/CMOS logic structure. Experimental results show that their advantages and disadvantages depend on the application being addressed. Finally, they also propose some design considerations and strategies to further optimize its reliability performance [5]. Breast cancer is a leading cause of suffering and death in women. The limitations of current diagnostic and therapeutic approaches have led to new strategies that positively impact survival and quality of life in breast cancer patients. Falagan-Lotsch et al. present an emerging approach based on actively targeted breast cancer nanomedicines. This approach uses a multifunctional inorganic nanoplatform with biomedical relevance, and nanotechnology offers real possibilities for reducing breast cancer mortality through early cancer detection, more precise diagnosis, and more effective treatment with minimal side effects [6]. The spread of antibiotic resistance and the growing prevalence of biofilm-associated infections are driving the need for new approaches to treating bacterial infections. Nanotechnology offers an innovative platform for addressing this challenge and even has the potential to manage infections involving multidrug-resistant (MDR) bacteria. Michal and Ehud summarize recent advances in the field of antimicrobial nanomedicines over the past few years and describes their unique properties, modes of action, and activities against MDR bacteria and biofilms and discusses biocompatibility and commercialization [7]. With the development of nanotechnology, there has been great interest in using nanomedicine strategies to enhance the radiation response of tumors. Nanomaterials containing high-Z elements to absorb radiation rays (such as X-rays) can act as radiosensitizers, depositing radiant energy within tumors and enhancing therapeutic efficacy. Song et al. believe that nanoscale carriers are capable of delivering therapeutic radioisotopes into tumors for internal RIT or delivering chemotherapeutic drugs to synergistically combined chemoradiotherapy. As revealed by recent studies, the tumor microenvironment can be modulated by various nanomedicine approaches to overcome hypoxia-related radioresistance. The tumor microenvironment means that the occurrence, growth, and metastasis of tumors are closely related to the internal and external environment of tumor cells. It not only includes the structure, function, and metabolism of the tumor tissue but also is related to the internal environment (nuclear and

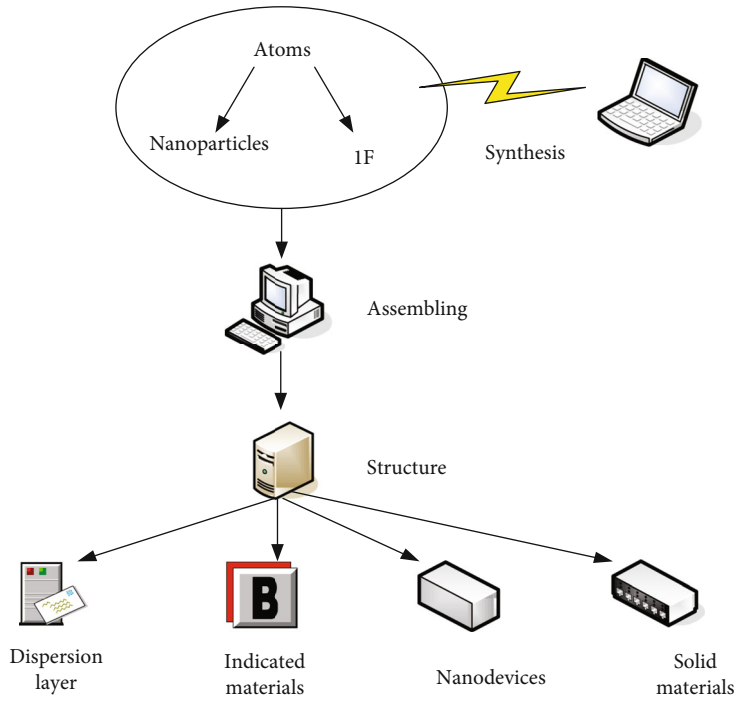

Figure 1: Nanomaterial structure.

cytoplasmic) of the tumor cell itself [8]. Although these theories describe nanotechnology and medical imaging, they are rarely combined and are not practical.

3. Nanotechnology and Medical Imaging Diagnostic Methods

3.1. Overview of Nanotechnology. Nanomaterials are materials with nanoscale structures, which can be divided into zero-dimensional nanomaterials and one-dimensional nanomaterials according to their specific dimensions. It has been asserted that when people can arrange and combine substances on a very small scale, they will obtain various novel materials [9, 10]. The change in properties caused by the ratio of the number of atoms on the surface of the nanocrystal particles to the total number of atoms increases sharply with the decrease of the particle size. For example, when the particle diameter is 10 nm, the particle contains 4000 atoms, and the surface atoms account for 40%; when the particle diameter is 1 nm, the particle contains 30 atoms, and the surface atoms account for 99%. Until the end of the last century, the first International Conference on Nanoscience and Technology was held in the United States, which formally combined theoretical research with contemporary science and technology, marking the official birth of nanotechnology [11]. When the size of the material is in the nanometer level, the number of atoms on the surface of the material will increase dramatically, which will far exceed the number of ordinary materials, and the chemical activity of the material will be greatly increased [12]. At the same time, nanomaterials are equal to or smaller than the wavelength of light wave, de Broglie wavelength and coherence length of superconducting state, and the periodic boundary of the material is destroyed, resulting in "novel" optical, electrical, magnetic, acoustic, and thermodynamic properties. In addition, nanomaterials also have quantum size effects and macroscopic quantum tunneling effects. These unique characteristics provide conditions for the wide-scale application of nanomaterials [13, 14]. Macroscopic quantum tunneling is one of the fundamental quantum phenomena, that is, when the total energy of a microscopic particle is less than the height of the potential barrier, the particle can still pass through the potential barrier. With the continuous and in-depth development of theory and practice, relatively systematic nanostructures have been established at present. With the maturity of application, the uniqueness of nanomaterials plays a pivotal role in the fields of biotechnology and advanced manufacturing [15, 16]. Nanorobots are the most tempting content in the application of nanotechnology in the medical field. They can act as miniature doctors in biomedical engineering and solve problems that are difficult for doctors to solve with traditional techniques. Figure 1 shows the nanomaterial structure.

Since the introduction of carbon fiber in the 1960s, it has become one of the widely used materials for composite materials due to its excellent characteristics such as high strength and high modulus and is widely used in the fields of structural materials and high-temperature materials, and it has the effect that other materials cannot match [17]. With the development of nanotechnology, researchers have applied nanotechnology to composite materials, specifically carbon fibers, and made them into new nanoreinforced materials. The material plays a pivotal role in the modification of polymer-based materials. In terms of specific functions, polymer-based materials have the advantages of two

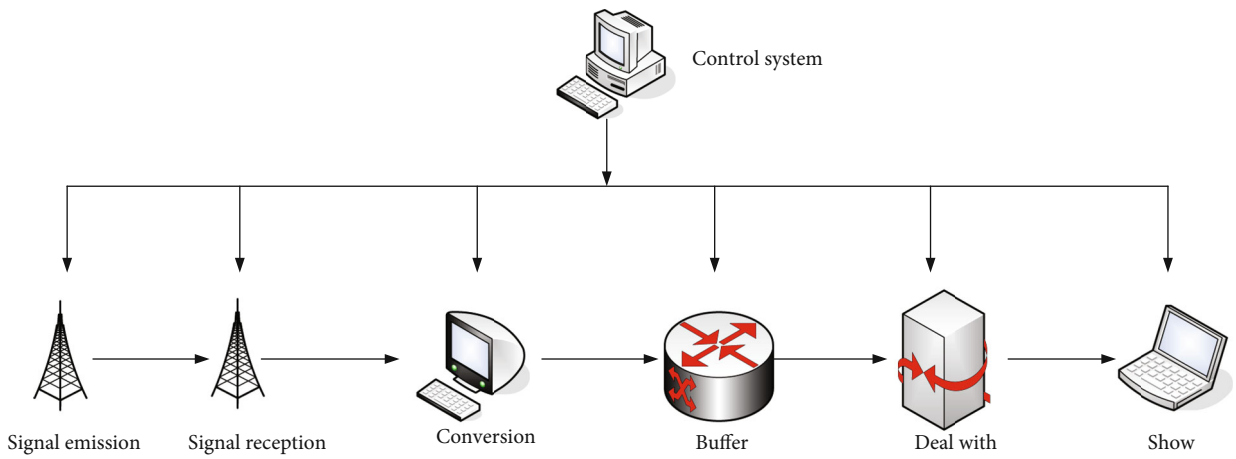

Figure 2: Ultrasonic flaw detector structure.

types of polymer materials, so they are nanocomposite materials with special performance materials [18, 19].

In the middle of the last century, the emergence of new substances made nanomaterials develop by leaps and bounds. In the subsequent gradual development, with the continuous exploration of theories by researchers, the scope of application of nanomaterials has become more and more extensive [20]. In recent years, the continuous improvement of science and technology has forced the upgrading of traditional materials. Traditional scientific and technological materials have been unable to meet the requirements of modern technology due to various functional limitations. New nanomaterials have a lot of room for development. From the offline situation, the entire nanomaterials are still in their infancy, and the follow-up development is still very violent. The focus of the first stage of development is to accurately control the number of atoms below 100. The second stage is the production of nanostructured substances, in which nanostructured substances and nanocomposites reach practical levels. In the third stage, it will be possible to mass-produce complex nanostructured substances. At this stage, although researchers choose different nanomaterials for experiments, so far there is no satisfactory result. In short, nanomaterials are very important functional materials, and the research and application of their properties still require continuous research and exploration [21, 22].

3.2. Image Processing Technology. Image processing refers to the process of analyzing images using computer technology [23]. Images are the basic tools for perception of the world and an important source of information for us. The subject of this article is the diagnosis and treatment of medical imaging. In the medical field, we often use imaging techniques, such as common B-ultrasound images and electrocardiograms [24, 25]. Therefore, it is necessary to focus on the research of image processing technology. Figure 2 shows the structure of the common ultrasound system.

In order to understand the information conveyed by the image, we need to collect data on the entire image. For the images collected by B-ultrasound, we need to process the B-ultrasound images because of external environmental interference during the acquisition process.

$$h(a) = k(a) * g_q + f_s. \tag{1}$$

Formula (1) represents the noise model, $k(a)$ represents the original image, $h(a)$ represents the actual image, and f_s represents the noise.

$$h(a) = k(a) * g_q. \tag{2}$$

In the process of image processing, if the various points of the image are connected, the diagnostic information can be more accurate. In this case, we define the functional expression of the digital image as

$$g(a,b) = \begin{bmatrix} g(1,1)\, g(1,2) \cdots g(1,n) \\ g(1,2)\, g(2,2) \cdots g(2,n) \\ \vdots \\ g(n,1)\, g(n,2)\, g(n,n) \end{bmatrix}, \tag{3}$$

where (a, b) represents a floating image point.

$$S_g(a,b) = y\big(S_g(g(a,b))\big). \tag{4}$$

$S_g(a, b)$ represents the gray value of the target point, g represents the displacement function of the image, and y represents the change function of the pixel value. The premise of pixel value transformation is spatial transformation, but this transformation does not occur in all cases. Figure 3 is a schematic diagram of image space conversion. When it changes, the function expression can be described as

$$S_g(a,b) = S_g(g(a,b)). \tag{5}$$

When formally transforming the image space, we need to determine the transformation process, especially the parameter transformation. We need to find the corresponding relationship

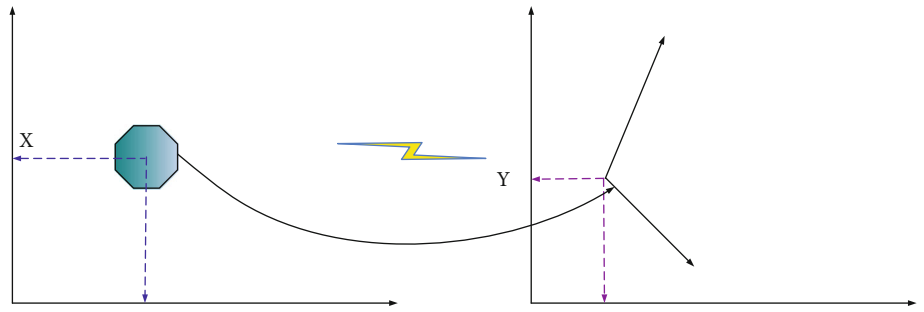

Figure 3: Principle of spatial transformation.

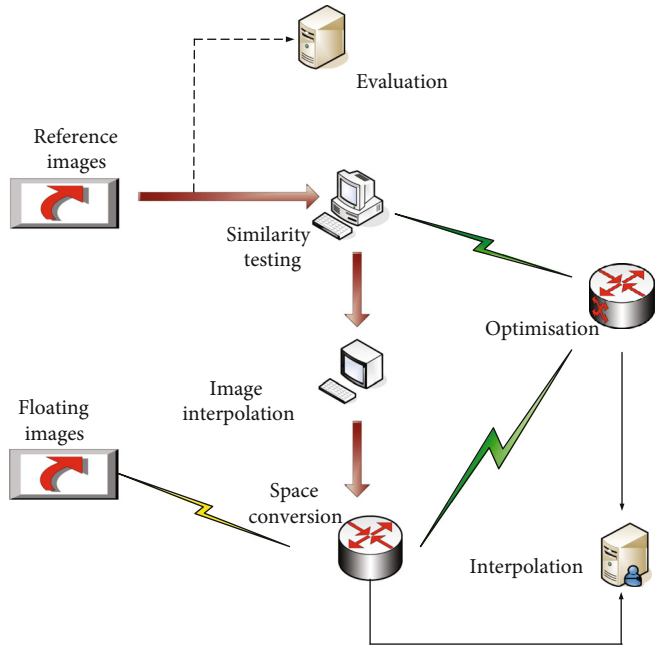

Figure 4: Image conversion process.

between the parameters. The main operation process is shown in Figure 4.

Entropy was originally used to represent the energy distribution in thermodynamics, and it has also made some progress in the medical field in recent years. We define its function expression as

$$F(a) = -q\sum_{i=1}^{m} k_i, \ln\left(k_i\right) \tag{6}$$

Among them, $\sum_{i=1}^{m} k_i = 1$, when $k1 = k2 = k3 = \cdots km$, F takes the maximum value.

$$Q(a) = \int_0^1 \left(Q_{\text{int}}(a) + Q_{\text{image}}(a)\right) dc, \tag{7}$$

where $Q_{\text{int}}(a)$ represents the internal energy, and its form is as follows:

$$Q_{\text{int}}(a) = \frac{1}{4}\left(\chi(c)\left|a'(c)\right|^3 + \eta(c)\left|a''(c)\right|^3\right). \tag{8}$$

Among them, $\chi(c)$ and $\eta(c)$ represent the weight coefficient.

In the process of image processing, entropy is mainly used to distinguish the foreground color and the background color. The main basis for distinguishing the foreground color and the background color is the gray value, and there is a big difference in the distribution of the gray value between the two. We express the expression of gray value as follows:

$$D_1(a) = -q\sum_{i=0}^{q-1} k_i \ln\left(k_i\right), \tag{9}$$

$$k(i) = \frac{g(i)}{\sum_{j=0}^{q-1} g(i)}. \tag{10}$$

Among them, $g(i)$ is the gray value function, q is a constant, and $k(i)$ represents the gray value range of 0–1.

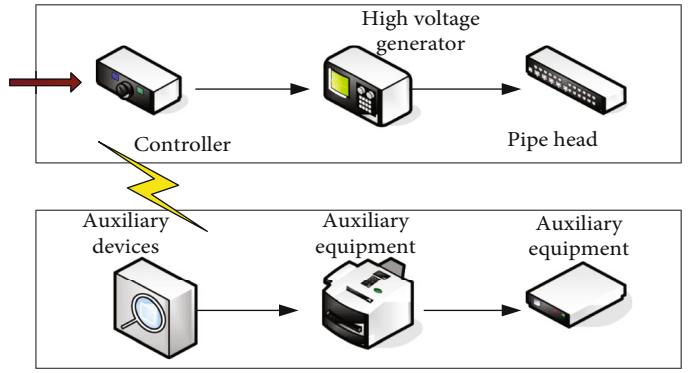

Figure 5: "X-ray" working principle.

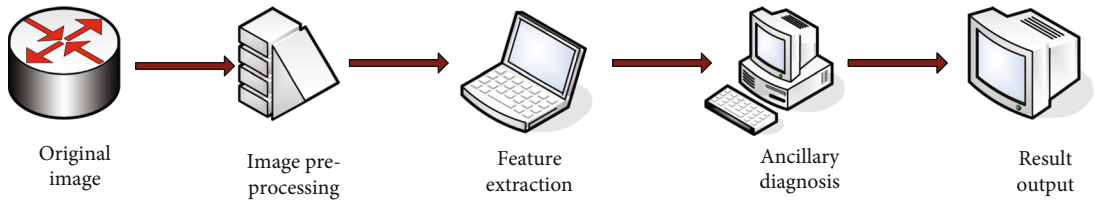

Figure 6: Image processing and diagnosis process.

The entropy of the part greater than the threshold q is expressed as

$$D_2(a) = -q\sum_{i=q}^{255} k_i \ln(k_i), \tag{11}$$

$$k(i) = \frac{g(i)}{\sum_{j=q}^{255} g(j)}. \tag{12}$$

Among them, $g(i)$ represents the gray value function, q is a constant, and $k(i)$ represents the gray value range in q-255.

The sum of the two entropies is

$$D(a) = D_1(a) + D_2(a). \tag{13}$$

When $D(a)$ is the largest, the threshold a is the maximum entropy threshold, that is, the threshold that distinguishes the foreground color from the background color.

$$\widehat{Q} = s * \bar{Q} + d * Q. \tag{14}$$

Formula (14) represents a filtering algorithm, which can suppress the formation of noise. $\widehat{Q}$ represents the image gray value, and Q represents the pixel gray value.

$$h(a,b) = \frac{\sum_{cd} t(c,d)u(a,b,c,d)}{\sum_{cd} u(a,b,c,d)}, \tag{15}$$

$$u(a,b,c,d) = \exp\left[-\left(\frac{(a-c)^3 + (j-d)^3}{\chi} + \frac{\|t(a,b) - u(c,d)\|}{\chi}\right)\right], \tag{16}$$

where χ represents the standard deviation of the intensity of the Gaussian function and formulas (15) and (16) represent the double filtering algorithm.

$$WY(a)(b) = \sum_p t(b,k)a(k) \tag{17}$$

Among them, $t(b,k)$ represents the weight coefficient, and a and b represent the pixels.

$$f(o,p) = \sum \|t(o) - u(p)\|_i^3, \tag{18}$$

$$f(o,p) = \sum k(j)\left(t(o_j) - u\left(p_j\right)\right). \tag{19}$$

i represents the standard deviation of the Gaussian function, and the value of $k(j)$ is determined according to the specific Gaussian function.

Smoothing the image is a very common technique. The gray value is calculated by calculating the weighted average value of the pixel points. The weighted average value is its core content, which is defined as

$$y(a) = \frac{u}{\partial\sqrt{2\pi}} e^{-(a-\varepsilon)^2/2\partial^2}. \tag{20}$$

Among them, the expected value of the Gaussian distribution is ε, the standard deviation is ∂, and the standard Gaussian distribution is $\varepsilon = 0, \partial = 1$.

In practical processing, we often use Gaussian blurred two-dimensional Gaussian distribution density distribution function, and its expression is expressed as

Table 1: Comparison of simulation results of PSNR image processing.

Simulation metrics	Category				
	1.2	0.9	0.6	0.3	0.1
Bayes threshold	52.93	52.03	48.72	47.22	42.63
Hard threshold	41.56	39.74	37.24	35.19	31.29
Soft threshold	37.01	36.28	34.71	32.47	28.31

Table 2: Comparison of simulation results of MMSIM image processing.

Simulation metrics	Category				
	1.2	0.9	0.6	0.3	0.1
Bayes threshold	0.998	0.995	0.992	0.989	0.984
Hard threshold	0.993	0.984	0.977	0.964	0.943
Soft threshold	0.982	0.982	0.973	0.947	0.921

$$H(a,b) = \frac{1}{2\pi\lambda^2} e^{-\left(a^2+b^2\right)/2\lambda^2}, \tag{21}$$

where λ represents the standard deviation.

3.3. Overview of Medical Imaging Equipment. Science benefits the world. With the continuous development of science and technology, medical technology is also constantly improving, and various medical imaging equipment has begun to be used in the medical field [26]. The "X-ray" we often hear is a typical imaging device. Due to the difference in tissue density and thickness of the human body, the X-ray measurement that passes through the inspected part will be absorbed to different degrees due to the difference in tissue density and thickness, and the final effect on the screen or film will be displayed as images with different degrees of blackening due to different measurement. In the mid-1890s, scientists discovered a ray that was invisible to the naked eye but had strong penetrating power during experiments. After continuous exploration, it is found that the ray can examine the internal mechanism of the object and display the outline of the internal organs. We can analyze and judge its health status through images [27, 28]. The working principle of "X-ray" is shown in Figure 5.

In order to save the image for a long time and use it more conveniently, we transmit the medical image information to the monitor, and the doctor can use the network to share the image resources and improve the work efficiency. At the same time, doctors can compare different imaging data of patients on the same device to improve the accuracy of diagnosis [29, 30]. When the image resources can be extracted on the device, the main purpose is to perform feature extraction; the purpose is to quantitatively analyze the lesion characteristics extracted in the first step, such as the size, density, and morphological characteristics of the lesion. At this time, we abandon the way of storing image data in the past, which saves management expenses to a certain extent, and at the same time facilitates access. Figure 6 shows the image processing and diagnosis flow [31].

Table 3: Imaging-related indicators.

Group	1	2	3	4
Number	65	60	80	70
Angle of abduction (°)	41	38	42	39
Proportion (%)	85	90	88	89
Anteversion angle (°)	22	18	17	19
Proportion (%)	76	88	87	89

Table 4: Image evaluation index analysis.

Projects		Clarity	Resolution
Group 1	Experimental group	17	0.9
	Original image	11	1.3
Group 2	Experimental group	16	0.9
	Original image	11	1.3

4. Application Experiments in Medical Imaging Diagnosis and Treatment

4.1. Image Processing Data. The image examination performed by the patient in the hospital must be processed to obtain the information transmitted by the image, and the doctor can prescribe the right medicine according to the information. The most important thing in image processing is to remove noise and signal effects. In fact, different thresholding will give different results, so I was able to experiment with images for different threshold ranges.

According to the data in Table 1, we have conducted experiments with different threshold processing schemes. First, we set the compression index as PSNR. When the noise parameter is 1.2, the Bayes threshold is 52.93, the hard threshold is 41.56, and the soft threshold is 37.01. When the noise parameter is 0.9, the Bayes threshold is 52.03, the hard threshold is 39.74, and the soft threshold is 36.28. When the noise parameter is 0.6, the Bayes threshold is 48.72, the hard threshold is 32.74, and the soft threshold is 34.71. When the noise parameter is 0.3, the Bayes threshold is 37.22, the hard threshold is 35.19, and the soft threshold is 32.47. When the noise parameter is 0.1, the Bayes threshold is 42.63, the hard threshold is 31.29, and the soft threshold is 28.31. According to the data, when different noise parameters are selected, the obtained image effects are different. Generally speaking, the larger the set range, the higher the threshold simulation index.

According to the data in Table 2, we set the compression index as MMSIM to conduct experiments with different threshold processing schemes. When the noise parameter is 1.2, the Bayes threshold is 0.998, the hard threshold is 0.993, and the soft threshold is 0.982. When the noise parameter is 0.9, the Bayes threshold is 0.995, the hard threshold is 0.984, and the soft threshold is 0.982. When the noise parameter is 0.6, the Bayes threshold is 0.992, the hard threshold is 0.977, and the soft threshold is 0.973. When the noise parameter is 0.3, the Bayes threshold is 0.989, the hard threshold is 0.964, and the soft threshold is 0.947. When the noise parameter is 0.1, the Bayes threshold

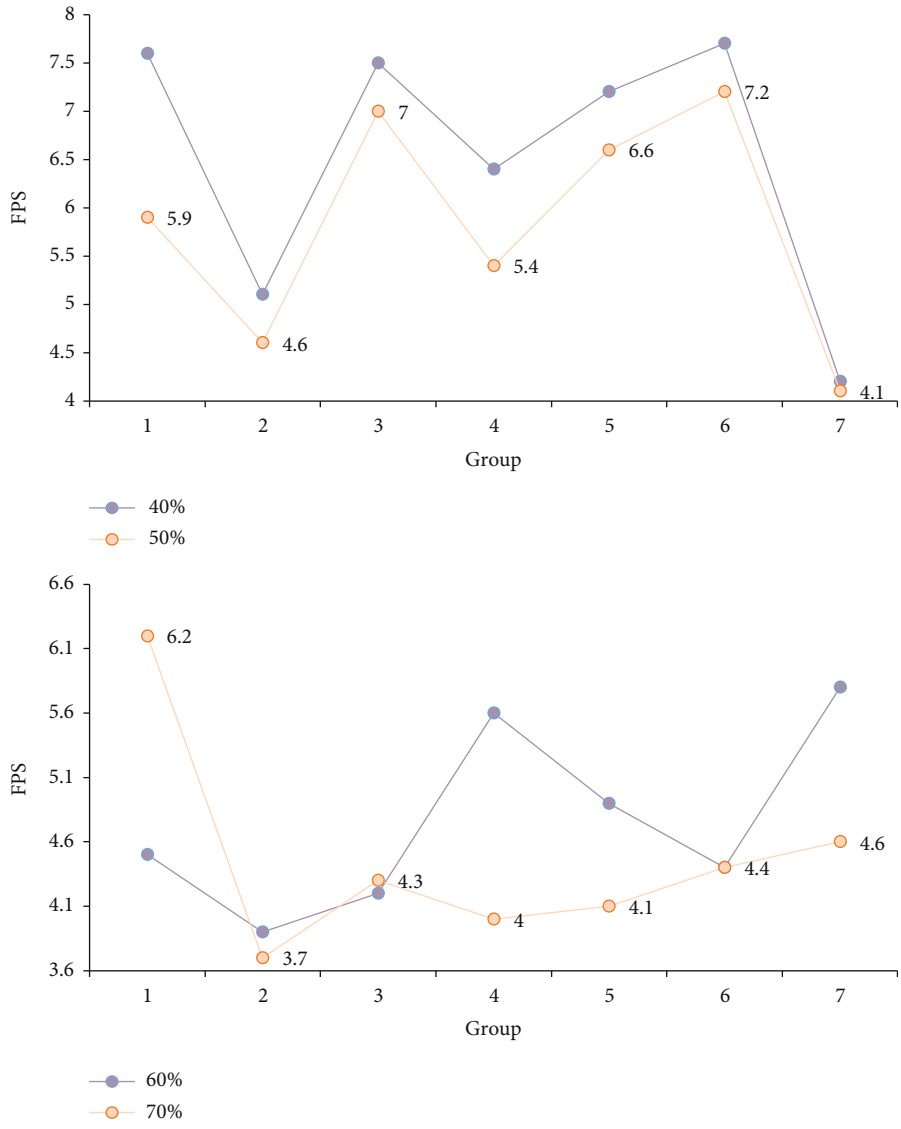

Figure 7: Different transmission image quality factor-MPR frame rate test results.

is 0.984, the hard threshold is 0.943, and the soft threshold is 0.921. According to the data, the optimal parameters can be selected according to different requirements during image noise reduction.

4.2. Imaging-Related Indicators. With the continuous development of science and technology, medical technology is also constantly improving. The development of imaging technology has promoted the progress of medical level. Based on this, we have briefly analyzed the relevant indicators of imaging. The details are as follows.

According to the data in Table 3, the abduction angle of the first group is 41°, the proportion in the safe area is 85%, the anteversion angle is 22°, and the proportion in the safe area is 76%. The second group had an abduction angle of 38°, 90% in the safe zone, and an anteversion angle of 18°, which was 88% in the safe zone. The third group had an abduction angle of 42°, 88% in the safe zone, and an anteversion angle of 17°, which was 87% in the safe zone. The fourth group had an abduction angle of 39°, 89% in the safe zone, and an anteversion angle of 19°, which was 89% in the safe zone.

4.3. Image Evaluation Metrics. After image processing, it needs to be evaluated; we usually use resolution and sharpness. In order to explore the effect of image processing, we compare and analyze the indicators of the processed image and the original image. The details are as follows.

According to the data in Table 4, we have conducted two sets of experiments when evaluating the image quality, and the clarity of the original image has reached level 11, and its resolution is 0.9. The first group of processed images has a sharpness of 17 levels and a resolution of 0.9. The second group of processed images has a sharpness of 16 levels and a resolution of 0.9. According to the data, the sharpness of the processed image is obviously improved, but the resolution is decreased, but in actual situation, it does not affect the diagnosis result. It can be

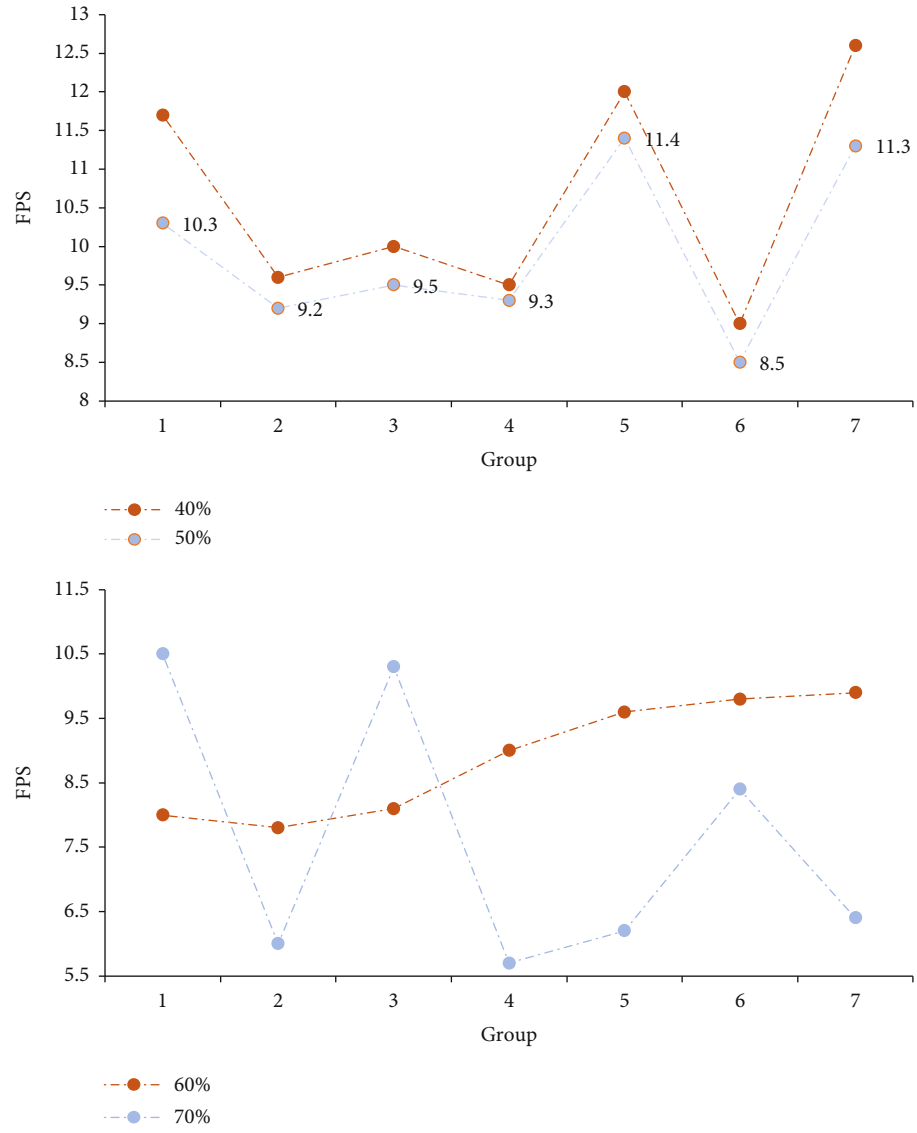

Figure 8: Different transmission image quality factor-DVR frame rate test results.

seen that the processed image is helpful for medical diagnosis [32].

5. Application Analysis of Medical Imaging Diagnosis and Treatment

5.1. Transmission Image Quality Factor System Performance Evaluation. Image quality is an important factor affecting doctors' diagnosis results, and the dynamic adjustment of image quality factors during image transmission has an important impact on image quality. When the user zooms and rotates the image, the original quality of the image will be reduced. For this reason, we briefly analyze the quality factor of image transmission. The details are as follows.

According to the data in Figure 7, we have carried out experimental analysis on the quality factor MPR frame rate in different ranges. At this time, the network environment of image transmission, network morbidity and image output device are all the same. In this case, we found that when the quality factor is 40%, the image transfer rate is 7.6FPS for the first time, 5.1FPS for the second time, and 7.5FPS for the third time. The image transmission rate of the fourth time is 6.4FPS, the image transmission rate of the fifth time is 7.2FPS, the image transmission rate of the sixth time is 7.7FPS, and the image transmission rate of the seventh time is 4.2FPS. When the quality factor is 50%, the first image transfer rate is 5.9FPS, the second image transfer rate is 4.6FPS, and the third image transfer rate is 7FPS. The image transmission rate of the fourth time is 5.4FPS, the image transmission rate of the fifth time is 6.6FPS, the image transmission rate of the sixth time is 7.2FPS, and the image transmission rate of the seventh time is 4.1FPS. According to the data, the smaller the image quality factor is, the larger the image transmission rate is generally, but the image transmission rate will fluctuate during the same type of transmission process.

In order to prevent the chance of the experimental data, we used different quality factors to carry out the comparison

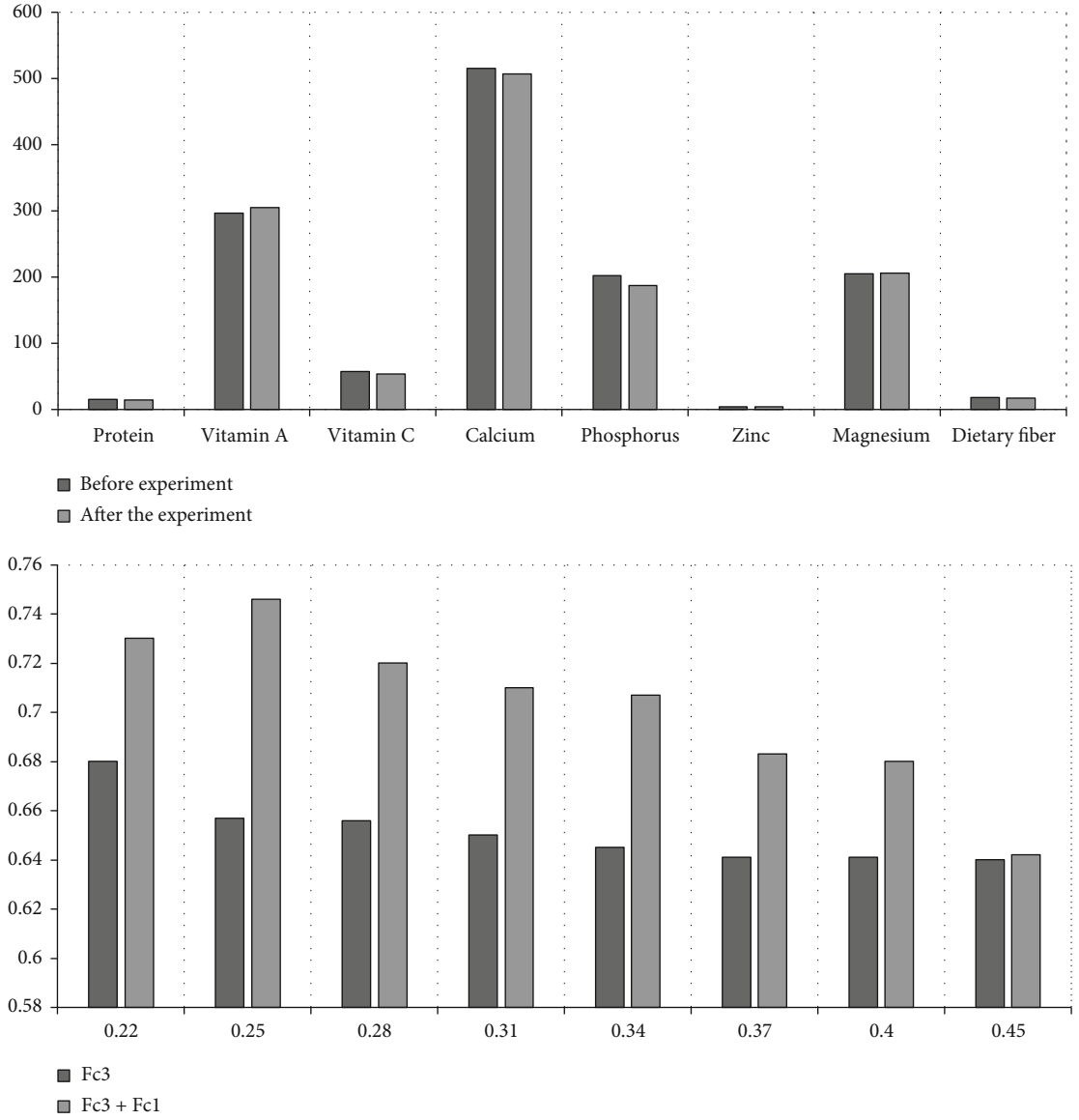

Figure 9: Image performance analysis.

experiment again. According to the trend of the experimental data, when the quality factor is 70%, the first image transmission rate is as high as 6.2FPS, and the subsequent transmission rate drops sharply. When the quality factor is 60%, its image transfer rate remains the same as in the previous experiment. It can be seen that the smaller the image quality factor is, the larger the image transmission rate is generally, but when the quality factor is 60%, the level is relatively middle [33].

According to the data in Figure 8, we have conducted experimental analysis on the quality factor of DVR frame rate in different ranges. At this time, the network environment of image transmission, network morbidity and image output device are all the same. In this case, we found that when the quality factor is 40%, the image transfer rate is 11.7FPS for the first time, 9.6FPS for the second time, and 10FPS for the third time. The image transmission rate of the fourth time is 9.5FPS, the image transmission rate of the fifth time is 12FPS, the image transmission rate of the sixth time is 9FPS, and the image transmission rate of the seventh time is 12.6FPS. When the quality factor is 50%, the first image transfer rate is 10.3FPS, the second image transfer rate is 9.2FPS, and the third image transfer rate is 9.5FPS. The image transmission rate of the fourth time is 9.3FPS, the image transmission rate of the fifth time is 11.4FPS, the image transmission rate of the sixth time is 8.5FPS, and the image transmission rate of the seventh time is 11.3FPS. According to the data, the smaller the image quality factor, the larger the image transmission rate, but the image transmission rate will fluctuate during the same type of transmission, which is the same as the MPR frame rate test result.

Similar to the DVR frame rate experiment, we conducted a second experimental comparison of DVR frame rate measurements. According to the data results, when the quality factor is 70%, the fluctuation of the image transmission rate

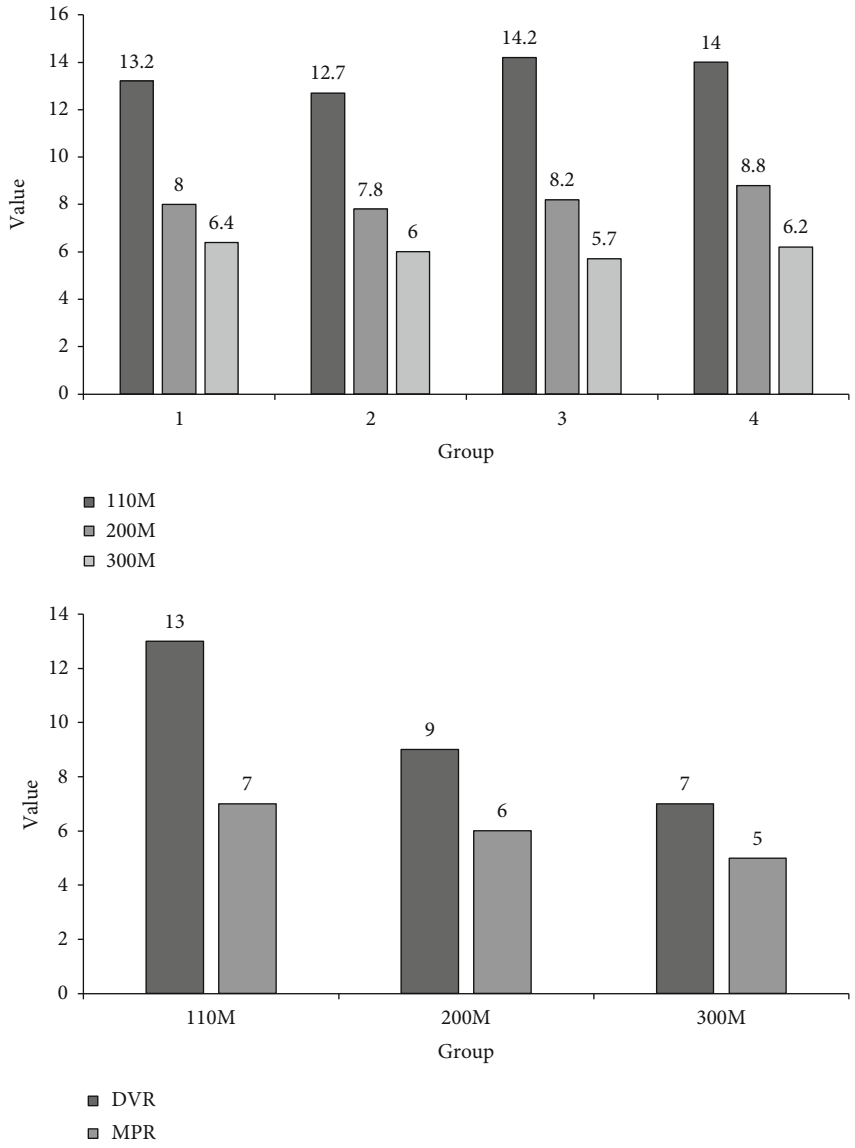

Figure 10: Image size data evaluation.

is too large, which is not suitable for image transmission. Secondly, according to the data, it can be found that when the quality factor is 60%, the fluctuation of the image transmission rate is small, which is suitable for image transmission.

5.2. Image Processing Performance Analysis. With the continuous development of imaging technology, medical imaging examination has become an indispensable inspection method in hospitals, providing strong support for clinical diagnosis and diagnosis. In order to explore the performance of image processing, we analyzed different situations of the image, as follows.

According to the data in Figure 9, this experiment retrieves the validity of medical images. When the usage rate of Fc1 was 22%, the image efficiency rate was 70%, and when the usage rate was 25%, the image efficiency rate was 69%. When the usage rate is 28%, the image efficiency rate is 68%, and when the usage rate is 31%, the image efficiency rate is 67.3%. When the usage rate is 34%, the image efficiency rate is 67%, and when the usage rate is 37%, the image efficiency rate is 60%. When the usage rate of Fc2 was 22%, the image efficiency rate was 68%, and when the usage rate was 25%, the image efficiency rate was 68.3%. When the usage rate is 28%, the image efficiency rate is 68.1%, and when the usage rate is 31%, the image efficiency rate is 67%. When the usage rate is 34%, the image efficiency rate is 66.5%, and when the usage rate is 37%, the image efficiency rate is 60%. According to this data, there is no significant difference in the imaging efficiency between Fc1 and Fc2.

When the usage rate of Fc3 was 22%, the image efficiency rate was 68%, and when the usage rate was 25%, the image efficiency rate was 65.7%. When the usage rate is 28%, the image efficiency rate is 65.6%, and when the usage rate is 31%, the image efficiency rate is 65%. When the usage

rate is 34%, the image efficiency rate is 64.5%, and when the usage rate is 37%, the image efficiency rate is 64.1%. When the combined use rate of Fc1 and Fc3 was 22%, the imaging efficiency rate was 73%, and when the utilization rate was 25%, the imaging efficiency rate was 74.6%. When the usage rate is 28%, the image efficiency rate is 72%, and when the usage rate is 31%, the image efficiency rate is 71%. When the usage rate is 34%, the image efficiency rate is 70.7%, and when the usage rate is 37%, the image efficiency rate is 68.3%. From this data, it can be seen that when Fc1 and Fc3 are used in combination, the imaging efficiency is greatly improved.

5.3. Image Size Data Evaluation. In addition to the transmission rate and the image quality factor, the image quality is also related to the size of the image itself. For this reason, we have analyzed images of different sizes. The details are as follows.

According to the data in Figure 10, we have conducted quality assessment on images of different data sizes. When the image is 110 M, the frame rate of the first test of the image is 13.2FPS, and the frame rate of the second test of the image is 12.7FPS. The frame rate of the third test of the image is 14.2FPS, and the frame rate of the fourth test of the image is 14FPS. When the image is 200 M, the frame rate of the first test of the image is 8FPS, and the frame rate of the second test of the image is 7.8FPS. The frame rate for the third test of the image was 8.2FPS, and the frame rate for the fourth test of the image was 8.8FPS. When the image is 300 M, the frame rate of the first test of the image is 6.4FPS, and the frame rate of the second test of the image is 6FPS. The frame rate for the third test of the image was 5.7FPS, and the frame rate for the fourth test of the image was 6.2FPS. When the size of the image data is the same, the DVR and MPR transmission rates of the images are quite different. According to the data, the size of the image data has a great influence on the image quality.

6. Conclusions

With the continuous progress of science and technology, the combination of science and technology and medical treatment has become the general trend. The continuous development of nanotechnology provides conditions for the development of the medical field. The purpose of this paper is to study the application of nanoscale microparticle technology in medical imaging diagnosis and treatment. It is expected that the combination of nanotechnology and medical imaging will improve the accuracy of medical imaging diagnosis. Although this paper has carried out some research on this basis, there are still some problems: the image processing method is very successful in the edge detection of the low-frequency part of the image, and the scale factor can be accurately calculated, but the sensitivity to the high-frequency part of the image is weak.

Data Availability

No data were used to support this study.

Conflicts of Interest

There is no potential conflict of interest in this study.

References

[1] Y. C. Lin, J. S. Wu, and J. W. Kung, "Image guided biopsy of musculoskeletal lesions with low diagnostic yield," *Current Medical Imaging Reviews*, vol. 13, no. 3, pp. 260–267, 2017.

[2] D. P. Frush and E. Sorantin, "Radiation use in diagnostic imaging in children: approaching the value of the pediatric radiology community," *Pediatric Radiology*, vol. 51, no. 4, pp. 532–543, 2021.

[3] S. Rpsgt, "Eliminating the stigma: a systematic review of the health effects of low-dose radiation within the diagnostic imaging department and its implications for the future of medical radiation," *Journal of Medical Imaging and Radiation Sciences*, vol. 51, no. 4, pp. 662–670, 2020.

[4] J. E. Venson, F. Bevilacqua, J. Berni, F. Onuki, and A. Maciel, "Diagnostic concordance between mobile interfaces and conventional workstations for emergency imaging assessment," *International Journal of Medical Informatics*, vol. 113, no. -MAY, pp. 1–8, 2018.

[5] E. Deng, W. Kang, and Y. Zhang, "Design optimization and analysis of multicontext STT-MTJ/CMOS logic circuits," *IEEE Transactions on Nanotechnology*, vol. 14, no. 1, pp. 169–177, 2015.

[6] P. Falagan-Lotsch, E. M. Grzincic, and C. J. Murphy, "New advances in nanotechnology-based diagnosis and therapeutics for breast cancer: an assessment of active-targeting inorganic nanoplatforms," *Bioconjugate Chemistry*, vol. 28, no. 1, pp. 135–152, 2017.

[7] M. Natan and E. Banin, "From nano to micro: using nanotechnology to combat microorganisms and their multidrug resistance," *FEMS Microbiology Reviews*, vol. 41, no. 3, pp. 302–322, 2017.

[8] G. Song, L. Cheng, and Y. Chao, "Emerging nanotechnology and advanced materials for cancer radiation therapy," *Advanced Materials*, vol. 29, no. 32, article 1700996, 2017.

[9] M. Bathe and P. Rothemund, "DNA nanotechnology: a foundation for programmable nanoscale materials," *MRS Bulletin*, vol. 42, no. 12, pp. 882–888, 2017.

[10] L. B. Naves, C. Dhand, J. R. Venugopal, L. Rajamani, S. Ramakrishna, and L. Almeida, "Nanotechnology for the treatment of melanoma skin cancer," *Progress in Biomaterials*, vol. 6, no. 1-2, pp. 13–26, 2017.

[11] D. Jasinski, F. Haque, D. W. Binzel, and P. Guo, "advancement of the emerging field of RNA nanotechnology," *ACS Nano*, vol. 11, no. 2, pp. 1142–1164, 2017.

[12] D. Lin, Y. Liu, and C. Yi, "Reviving the lithium metal anode for high-energy batteries," *Nature Nanotechnology*, vol. 12, no. 3, pp. 194–206, 2017.

[13] P. Senellart, G. Solomon, and A. White, "High-performance semiconductor quantum-dot single-photon sources," *Nature Nanotechnology*, vol. 12, no. 11, pp. 1026–1039, 2017.

[14] E. C. Yusko, B. R. Bruhn, O. M. Eggenberger et al., "Real-time shape approximation and fingerprinting of single proteins using a nanopore," *Nature Nanotechnology*, vol. 12, no. 4, pp. 360–367, 2017.

[15] C. Y. Chen, C. M. Wang, H. H. Li, H. H. Chan, and W. S. Liao, "Wafer-scale bioactive substrate patterning by chemical lift-off

lithography," *Beilstein Journal of Nanotechnology*, vol. 9, no. 1, pp. 311–320, 2018.

[16] L. Wang, M. Boutilier, P. R. Kidambi, D. Jang, N. G. Hadjiconstantinou, and R. Karnik, "Fundamental transport mechanisms, fabrication and potential applications of nanoporous atomically thin membranes," *Nature Nanotechnology*, vol. 12, no. 6, pp. 509–522, 2017.

[17] M. Hadjidemetriou and K. Kostarelos, "Evolution of the nanoparticle corona," *Nature Nanotechnology*, vol. 12, no. 4, pp. 288–290, 2017.

[18] F. Pi, Z. Hui, and L. Hui, "RNA nanoparticles harboring annexin A2 aptamer can target ovarian cancer for tumor-specific doxorubicin delivery," *Nanomedicine: Nanotechnology, Biology, and Medicine*, vol. 13, no. 3, pp. 1183–1193, 2017.

[19] M. Holzinger, R. Haddad, and A. Maaref, "Amperometric biosensors based on biotinylated single-walled carbon nanotubes," *Journal of Nanoscience & Nanotechnology*, vol. 9, no. 10, pp. 6042–6046, 2009.

[20] Y. Weng, J. Liu, S. Jin, W. Guo, X. Liang, and Z. Hu, "Nanotechnology-based strategies for treatment of ocular disease," *Acta Pharmaceutica Sinica B*, vol. 7, no. 3, pp. 281–291, 2017.

[21] C. A. Mirkin, T. J. Meade, and S. H. Petrosko, "Nanotechnology-based precision tools for the detection and treatment of cancer," *Anticancer Research*, vol. 35, no. 10, pp. 481–501, 2017.

[22] C. P. Reis and C. Damgé, "Nanotechnology as a promising strategy for alternative routes of insulin delivery," *Methods in Enzymology*, vol. 508, no. 508, pp. 271–294, 2017.

[23] C. H. Lee, B. Tiwari, D. Zhang, and Y. K. Yap, "Water purification: oil–water separation by nanotechnology and environmental concerns," *Environmental Science Nano*, vol. 4, no. 3, pp. 514–525, 2017.

[24] J. S. Duhan, R. Kumar, N. Kumar, P. Kaur, K. Nehra, and S. Duhan, "Nanotechnology: the new perspective in precision agriculture," *Biotechnology Reports*, vol. 15, no. 15, pp. 11–23, 2017.

[25] M. C. Roco, C. A. Mirkin, M. C. Hersam, and C. S. Alrokayan, "Nanotechnology research directions for societal needs in 2020," *Journal of Nanoparticle Research*, vol. 13, no. 3, pp. 897–919, 2018.

[26] Group, SFR-IA and French Radiology Community, "Artificial intelligence and medical imaging 2018: French Radiology Community white paper," *Imaging*, vol. 99, no. 11, pp. 727–742, 2018.

[27] X. Yi, H. Li, and A. Hcc, "Clinical placements for undergraduate diagnostic radiography students amidst the COVID-19 pandemic in Singapore: preparation, challenges and strategies for safe resumption," *Journal of Medical Imaging and Radiation Sciences*, vol. 51, no. 4, pp. 560–566, 2020.

[28] B. Jppa, E. Alcd, and G. Lbf, "Tomorrow's medical imaging builds on today's foundations - prevention, care and innovation at the service of patients: a program for radiology and medical imaging-ScienceDirect," *Diagnostic and Interventional Imaging*, vol. 101, no. 3, pp. 123–125, 2020.

[29] D. Mcrobbie, "Both sides now: diagnostic imaging medical physics in two hemispheres," *Australasian Physical & Engineering Sciences in Medicine*, vol. 40, no. 2, pp. 269–272, 2017.

[30] C. L. Ramanujam, D. Han, and T. Zgonis, "Medical imaging and laboratory analysis of diagnostic accuracy in 107 consecutive hospitalized patients with diabetic foot osteomyelitis and partial foot amputations," *Foot & Ankle Specialist*, vol. 11, no. 5, pp. 433–443, 2018.

[31] Jabbar Abed Eleiwy, "Characterizing wavelet coefficients with decomposition for medical images," *Journal of Intelligent Systems and Internet of Things*, vol. 2, no. 1, pp. 26–32, 2021.

[32] I. Mohammed, "Alghamdi, neutrosophic set with adaptive neuro-fuzzy inference system for liver tumor segmentation and classification model, International Journal of Neutrosophic," *Science*, vol. 18, no. 2, pp. 174–185, 2022.

[33] F. Q. Kareem and A. M. Abdulazeez, "Ultrasound medical images classification based on deep learning algorithms: a review, Fusion: Practice and Applications," vol. 3, no. 1, pp. 29–42, 2021.